Catalysis Today 141 (2009) 161–167

Contents lists available at ScienceDirect

Catalysis Today

journal homepage: www.elsevier.com/locate/cattod

Ru(II)-Chiral (1*R*,2*S*)-(+)-*cis*-1-amino-2-indanol immobilized over SBA-15 for asymmetric transfer hydrogenation reaction of prochiral ketones

Surendran Parambadath, A.P. Singh [*]

Inorganic and Catalysis Division, National Chemical Laboratory, Pune 411008, India

ARTICLE INFO

Article history:
Available online 7 July 2008

Keywords:
Mesoporous molecular sieve
SBA-15
Chiral amino alcohols
(1*R*,2*S*)-(+)-*cis*-1-amino-2-indanol
Asymmetric transfer hydrogenation
Prochiral ketones

ABSTRACT

Mesoporous SBA-15 (Santa Barbara University at California) has been synthesized and functionalized with (4-chloromethyl)phenyltriethoxysilane, there after the surface silanols groups were passivated by dimethoxydimethylsilane (MeO_2Me_2Si) [Bz-SBA-15]. Further (1*R*,2*S*)-(+)-*cis*-1-amino-2-indanol [AIL] has been immobilized over functionalized SBA-15 (BzAIL-SBA-15). The heterogeneous catalysts were synthesized by complexation of BzAIL-SBA-15 by $[RuCl_2(benzene)]_2$ and $[RuCl_2(p\text{-cymene})]_2$ in 2-propanol at reflux condition designated as Ru-Bn-BzAIL-SBA-15 (**Ru-1**) and Ru-Cy-BzAIL-SBA-15 (**Ru-2**). The synthesized materials have been characterized by small angle X-ray diffraction spectroscopy (SAXS), N_2 adsorption–desorption isotherms, Fourier Transformed-Infra-red (FT-IR) spectroscopy, Transmission Electron Microscopy (TEM), intensively coupled plasma atomic emission spectroscopy (ICP-AES), Diffuse reflectance UV–vis and ^{13}C CP MAS NMR analysis. Further the synthesized and characterized materials (**Ru-1** and **Ru-2**) have been successfully applied in the asymmetric transfer hydrogenation (ATH) reaction of simple prochiral ketones, which gave a yield of 56% and 18% and enantiomeric excess (ee) values of 62% and 77% for **Ru-1** and **Ru-2**, respectively, after 1 h for acetophenone. The reusability studies showed approximately the same enantiomeric excess value at lower conversions.

1. Introduction

The enantioselective transfer hydrogenation of ketones and imines has been considered as an efficient method for the synthesis of chiral secondary alcohols or amines with high enantiomeric purity emerging as a topic of intense research due to the mild reaction conditions, operational simplicity, low fractional yields of side products and high product yields in high enantiomeric purity. The discovery of ruthenium (II) complex with Ts-DPEN [(*R*,*R*)- or (*S*,*S*)-N-(*p*-toluenesulphonyl)-1,2-diphenylethylene diamine] reported by Noyori and co-workers [1] was the real milestone for the development of this area as a universal interest. But the homogenic nature of many of such type complexes limits the wide utility in industrial processes. To avoid this situation, immobilization to the surface of silica like zeolites, mesoporous silicas, layered clays or a polymer, has been more attracted in these attempts because of the comparable activity and enantioselectivity with its homogenous analogous. For silica support simple filtration or centrifugation is enough to separate the highly precious metal catalyst and for polymer the recycling by reprecipitation by the addition of suitable solvents to the reaction mixture after use [2]. Mesoporous materials can offer many attractive features for the heterogenization of homogeneous complexes including uniform large pore size, high surface area, insolubility in organic solvents and inert to many chemical substrates. The real covalently anchored heterogeneous analogous of Noyori's catalyst was introduced by Y.Q. Tu and co-workers [3,4] on amorphous silica gel, mesoporous MCM-41 and SBA-15 for asymmetric transfer hydrogenation (ATH) of various ketones in water, which demonstrated excellent enantioselectivities (up to >99% ee) and very high reactivities (>99% yield within 2–8 h) with and with out an additive.

Ru(II), Rh(III) and Ir(III) complexes of β-amino alcohols also reported as efficient catalysts for the asymmetric transfer hydrogenation reaction of aromatic ketones in 2-propanol. There are only a few reports on the use of homogeneous [5–7] and heterogeneous [8–10] chiral Ru^{II} amino alcohols complexes as catalysts despite some interesting approaches recently reported which concerns the anchoring of transfer hydrogenation catalysts onto organic supports. The uses of inorganic amorphous and mesoporous silica supports for the preparation of ATH catalysts are still rare. A new series of covalently anchored Ru^{II} catalysts on the surface of amorphous silica have been reported by Reek et al. [11] using (4-chloromethyl)phenyltriethoxy silane as tethering agent

---

[*] Corresponding author. Tel.: +91 25902633; fax: +91 25902633.
E-mail address: ap.singh@ncl.res.in (A.P. Singh).

0920-5861/$ – see front matter © 2008 Elsevier B.V. All rights reserved.
doi:10.1016/j.cattod.2008.04.003

for ATH of acetophenone. To the best of our knowledge no reports are available to date by the use of covalently anchored Ru(II)-(1*R*,2*S*)-(+)-*cis*-1-amino-2-indanol over amorphous or mesoporous silica as catalyst for ATH of prochiral ketones.

Here, we report, the synthesis, characterization and catalytic applications of covalently anchored heterogeneous Ru(II) catalyst systems derived from a chiral (1*R*,2*S*)-(+)-*cis*-1-amino-2-indanol for asymmetric transfer hydrogenation of simple ketones. We have also described a detailed characterization to clear out the unambiguity of the functionalization, ligand immobilization and anchoring of metal complexes over mesoporous solid support. The performance of the catalysts was tested in the asymmetric transfer hydrogenation of simple prochiral ketones.

2. Experimental

2.1. Compounds and materials

Tetraethylorthosilicate (TEOS), Pluronic P123, (1*R*,2*S*)-(+)-*cis*-1-amino-2-indanol, all ketones and $[RuCl_2(p\text{-cymene})]_2$ were purchased from Aldrich chemicals (USA). $[RuCl_2(benzene)]_2$ was synthesized according to a literature procedure [12]. The reagent grade solvents were obtained from Merck (India) and dried before use according to standard methods. HPLC grade 2-propanol was used for reaction.

2.2. Synthesis of siliceous SBA-15 (1)

SBA-15 was synthesized following a similar procedure reported in literature [13] with slight modification. The SBA-15 used in this paper has been synthesized from a typical synthesis batch with the composition of 4.4 g Pluronic P123 $M_{avgerage} = 5800$ [EO_{20}-PO_{70}-EO_{20}], 120 g of 2M HCl and 9 g TEOS. Typically 4.4 g of triblock co-polymer was dispersed in 30 g-distilled water and stirred for 1.5 h. To the resultant solution, 120 g of 2M HCl was added under stirring and the stirring was continued for 2 h. Finally, 9 g of TEOS was added drop wise and the mixture was maintained at 35 °C for 24 h without stirring. The resulted heterogeneous mixture was submitted to hydrothermal treatment at 100 °C for 48 h under static condition before recovering the solid material. The crystallized product was filtered, washed with distilled water and dried in air for 12 h and in oven at 70 °C for 12 h and then calcined at 450 °C for 8 h in air to remove the template completely. The structure was confirmed by XRD and surface area.

2.3. Modification of SBA-15 using 4-chloromethylphenyltriethoxysilane, Bz-SBA-15 (**2**)

1 g of calcined SBA-15 in 30 ml dry toluene was refluxed with the required amount of (4-chloromethyl)phenyltriethoxysilane for 36 h under inert atmosphere. The material was filtered after cooling to ambient temperature, washed with dry toluene and then with dichloromethane. Soxhlet extraction was carried out for 24 h in dichloromethane to remove unattached functional molecules. The sample was dried in vacuum for 10 h. The dried material (BzCl-SBA-15) was stirred with excess of dimethoxydimethylsilane (MeO_2-Me_2Si) in dry toluene for 24 h under reflux condition to passivate the undisturbed silanol groups inside and out side the porous material. The filtered sample was washed with dichloromethane several times and dried under vacuum for 10 h. The resulted organo-functionalized material was designated as Bz-SBA-15 (**2**).

2.4. Ligand functionalization of SBA-15, BzAIL-SBA-15 (3)

To Bz-SBA-15 (1 g) in 30 ml dry toluene, added a mixture of triethylamine (0.4 ml) and (1*R*,2*S*)-(+)-*cis*-1-amino-2-indanol (1.83 mmol, 0.275 g). The whole mixture was stirred for 24 h under reflux condition and under inert atmosphere. The resulted material was filtered and washed initially with dry toluene and after a 1:1 mixture of dichloromethane and methanol. The material was then stirred in 1:1 dichloromethane/methanol (100 ml) mixture for 2 h at room temperature, filtered, washed with dichloromethane and dried in vacuum for 10 h. The resultened material was named as BzAIL-SBA-15 (**3**) (Scheme 1).

2.5. Anchoring of $[Ru^{II}Cl_2(benzene)]_2$/$[Ru^{II}Cl_2(p\text{-cymene})]_2$ inside ligand functionalized SBA-15

30 mg of $[Ru^{II}Cl_2(benzene)]_2$/$[Ru^{II}Cl_2(p\text{-cymene})]_2$ was taken in 40 ml of dry 2-propanol containing 0.15 ml triethylamine (Net_3)

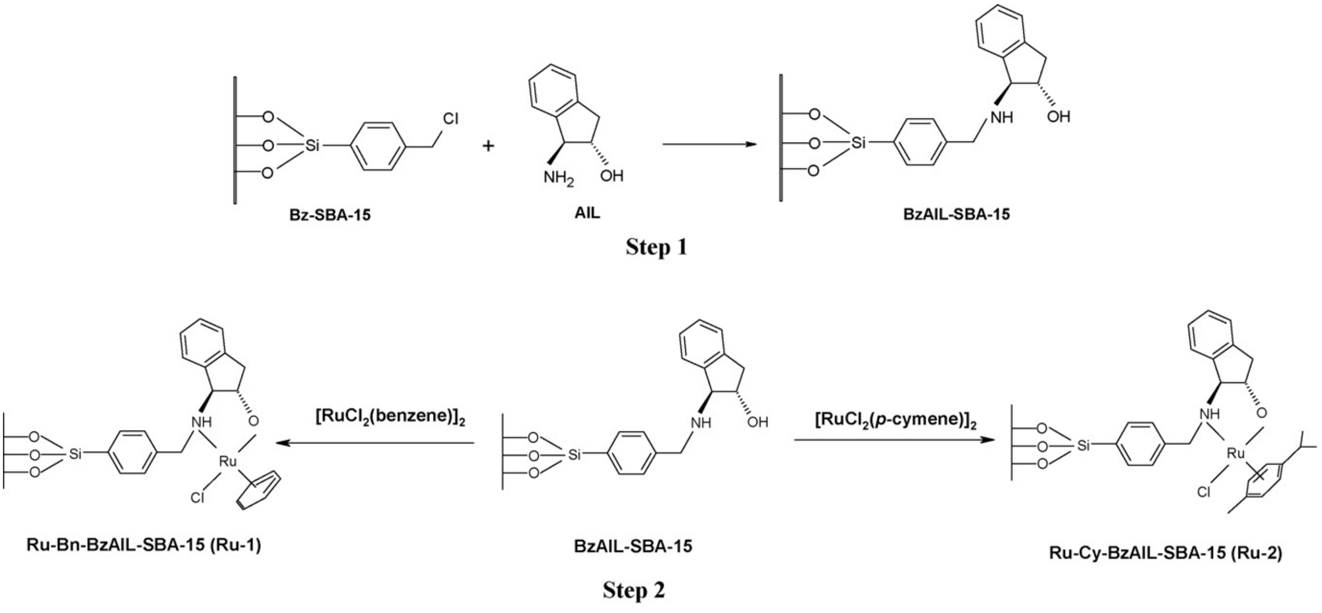

Scheme 1. Synthetic approach to SBA-15 immobilized Ru(II)-(1*R*,2*S*)-(+)-*cis*-1-amino-2-indanol complexes. (Step 1) Immobilization of (1*R*,2*S*)-(+)-*cis*-1-amino-2-indanol; (Step 2) Preparation of **Ru-1** and **Ru-2**.

and refluxed for 1 h under inert condition with stirring after the addition of 1 g of (**3**). The final brown solid was filtered off and washed with dry 2-propanol for several times, then dried under vacuum for 12 h at 50°C. The synthesized materials were named as Ru-Bn-BzAIL-SBA-15 (**Ru-1**), {catalyst prepared from [$Ru^{II}Cl_2$(benzene)]$_2$} and Ru-Cy-BzAIL-SBA-15 (**Ru-2**), {catalyst prepared from [$Ru^{II}Cl_2$(*p*-cymene)]$_2$} (Scheme 1).

2.6. Catalyst characterization

In order to identify the structure, phase purity, degree of crystallinity, unit cell parameters the powder small angle X-ray diffraction analysis was done on a SIEMENS D5005 diffractometer using Cu Kα (λ = 0.154 nm) radiation. The specific surface areas of the samples were determined by the BET method from N_2 adsorption isotherms at −196 °C using an Omnisorb CX-100 Coulter instrument. Before measuring the surface area, the samples were activated at 120 °C for 3 h under nitrogen atmosphere. The elemental analyses were done with an EA1108 CHN/S Elemental Analyzer (Carlo Erba Instrument) for establishing the presence and exact fraction of elements in the synthesized materials. Diffuse reflectance UV–vis spectra of the powder samples were recorded in the range 200–800 nm on Shimadzu UV 2101 PC spectrometer equipped with a diffuse reflectance attachment, using $BaSO_4$ as the reference. The metal loading was found with an inductive couple plasma atomic emission spectroscopy (ICP-AES) on a spectroflame D (Spectro analytic instrument). A Shimadzu FT-IR 8201 PC Diffuse Reflectance Scanning disc technique was used to probe the attached groups and nature of the surface functional groups in the material. 125.757 MHz solid-state ^{13}CP MAS NMR studies were carried out on a Bruker DRX-300 NMR spectrometer. The spectrum was recorded under Hartmann-Hahn match condition using a contact time of 1 m/s and a relaxation delay of 4 s. The TEM observations were made using a JEOL-JEM-1200 EX instrument with 120 kV of acceleration voltage to probe the presence of hexagonal mesophase in the extracted material. Reactions were monitored by TLC using aluminum-backed silica gel 60 (F_{254}) plates, visualized using $UV_{254\ nm}$ and PMA dip. The catalytic activity and enantiomeric excess (ee) were measured on an HP 6890 gas chromatograph equipped with a flame ionization detector and a HP-Chiral 30 m β-cyclodextrin capillary column (30 m × 0.32 mm × 0.25 μm).

2.7. General reaction procedure for heterogeneous Ru (II) catalyzed asymmetric transfer hydrogenation of ketones in 2-propanol

0.0001 mol.% (Ru content) of the catalyst (**Ru-1**/**Ru-2**) was taken in a round bottom flask having 3 ml of dry 2-propanol and degassed three times with N_2. The required amount of ketone (0.01 mol.%) by a syringe followed by KOH (3 mg) in 2-propanol (0.3 ml) was added under inert condition. The reaction mixture was stirred at 60 °C for an appropriate time and there after quenched by the addition of NH_4Cl (10 ml, saturated aqueous solution). After filtration, reaction mixture was washed subsequently with saturated $NaHCO_3$, saturated brine solution and water and the organic layer was separated by using diethyl ether. The residue was purified by a short silica gel column after saturation at high vacuum, eluted by petroleum ether/ethyl acetate (9:1). Reduced the volume, yield and enantiomeric excess were determined by GC analysis. We have used a HP 6890 gas chromatograph equipped with a flame ionization detector and an HP-Chiral 30 m β-cyclodextrin capillary column (30 m × 0.32 mm × 0.25 μm) (Scheme 2).

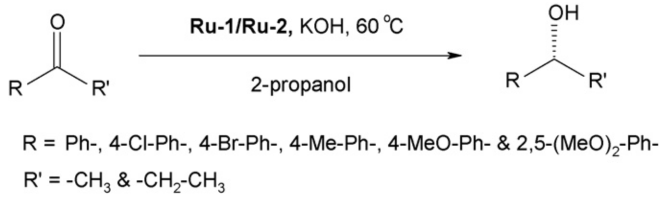

Scheme 2. Asymmetric transfer hydrogenation of simple prochiral ketones in 2-propanol.

3. Results and discussion

3.1. Powder X-ray diffraction

Fig. 1 shows the small angle powder XRD patterns recorded from (a) calcined SBA-15 (b) Bz-SBA-15 (c) BzAIL-SBA-15 (d) (**Ru-1**) and (e) (**Ru-2**) samples, in which a strong reflection for all patterns at 2θ value 0.906 indicates a well-pronounced (1 0 0) reflection. Two additional peaks were observed in all samples at 2θ values 1.51 and 1.75 corresponding to (1 1 0) and (2 0 0) reflections, which can be indexed for a structurally well-ordered hexagonal, lattice reflections and thus verifying that these samples are typical of hexagonal SBA-15-type materials prepared at pH ≤2 [13]. In all the samples, (1 1 0) reflection is more intense than the (2 0 0) reflection. It favors the more complete condensation of the wall structure due to the higher temperatures preferring at hydrothermal synthesis and further calcination. From this it is confirmed that the calcined SBA-15 material has a stable pore wall thickness to retain its integrity even after several modification treatments. A negligible decrease in peak intensities to the (1 0 0), (1 1 0) and (2 0 0) reflections was observed by functionalization followed by immobilization of ligand and further complexation with ruthenium precursors. This minor loss indicates that, even the presence of a large amount of organic moieties by the partial filling inside the mesopores is less detrimental to the quality of the SBA-15 material. The persistence of the (1 0 0), (1 1 0) and (2 0 0) reflections not only proved the structural stability and existence of long-range ordering to the mesophase but also the survival of undisturbed pore wall thickness even after a number of treatments with organic molecules in solvents under radical conditions. All the

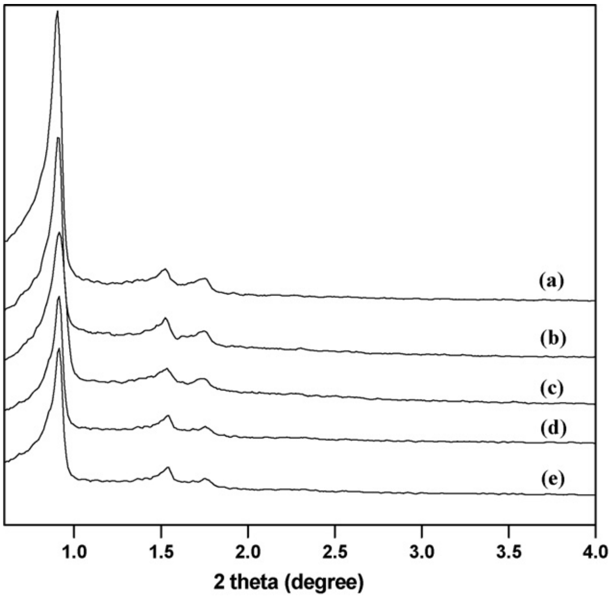

Fig. 1. Low angle XRD patterns of (a) SBA-15, (b) Bz-SBA-15, (c) BzAIL-SBA-15, (d) **Ru-1** and (e) **Ru-2**.

Table 1
Physico-chemical properties of synthesized catalysts

Material	% of Ru[a] (w/w)	BET adsorption–desorption measurements[b]		
		Surface area ($m^2\ g^{-1}$)	Pore diameter (Å)	Pore volume ($cm^3\ g^{-1}$)
SBA-15	–	854	78	1.16
Bz-SBA-15	–	610	73	0.80
BzAIL-SBA-15	–	501	71	0.68
Ru-1	0.45	459	70	0.59
Ru-2	0.46	456	70	0.59

[a] Analyzed by ICP-AES to measure the total metal complex loading (Wt/g in 100 g of heterogeneous catalyst).
[b] Measured by N_2 adsorption–desorption at −196 °C.

observations clearly show that the ordered mesoporosity and structural stability of the samples have retained after incorporation of organometallic complexes.

3.2. N_2 sorption studies

N_2 sorption isotherms were measured for the pure support and for the immobilized complexes, represent a comparison of sorption isotherms and textural characteristics of pure and immobilized catalyst samples (Table 1). All the materials displayed type IV isotherm (definition by IUPAC) with H_1-type hysteresis that is typical of mesoporous materials with cylindrical channels possessing pore diameters between 2 and 50 nm [13]. Calcined SBA-15 material has a Brunauer–Emmett–Teller (BET) surface area of 854 $m^2\ g^{-1}$ and a pore volume of 1.16 $cm^3\ g^{-1}$. The surface area values of Bz-SBA-15, BzAIL-SBA-15, (**Ru-1**) and (**Ru-2**) are 610, 501, 459 and 456 $m^2\ g^{-1}$, respectively. These samples showed a dramatic decrease in surface area on progressing the surface modification process and the ligand-modified samples obviously exhibit lower specific surfaces than the parent solids due to the introduction of the organic moieties (functional group/Me_2Si-/ligands), which is also responsible for a reduction of pore volumes and pore diameters. A specific surface area decrease from 854 to 610 $m^2\ g^{-1}$ (about 28% decrease) while functionalization and further passivation of hydroxyl groups of calcined SBA-15 clearly point out the anchoring of a considerable amount of tethering molecule inside the pores of calcined silica support. A further but small decrease in surface area for BzAIL-SBA-15 (501 $m^2\ g^{-1}$) is due to the ligand immobilization over Bz-SBA-15. The decreased specific surface areas for **(Ru-1)** and **(Ru-2)** *ca.* 459 and 456 $m^2\ g^{-1}$, respectively, clearly indicate the successful complexation of the immobilized ligands by ruthenium precursors. Nearly similar surface area values are obtained for **Ru-1** and **Ru-2** indicates an agreement in metal loading in both the heterogeneous catalysts.

Table 1 represents the average pore diameters of calcined SBA-15 (78 Å), Bz-SBA-15 (73 Å), BzAIL-SBA-15 (71 Å) and 70 Å (**Ru-1/Ru-2**). It is observed that a decrease in average pore diameter from 78 Å (calcined SBA-15) to 70 Å (**Ru-1/Ru-2**) is due to the functionalization, ligand immobilization and further complexation processes. From the pore size distribution, we have observed a narrow pore size distributions for the parent solid SBA-15 (Figure not given) but for the modified materials, broad and lower pore size distributions were obtained (73–70 Å), which might imply that the chelating ligand and the Me_2Si-groups are not uniformly distributed through the SBA-15 channel surface in these samples [14].

The pore volumes of calcined SBA-15 (1.16 $cm^3\ g^{-1}$), Bz-SBA-15 (0.80 $cm^3\ g^{-1}$), BzAIL-SBA-15 (0.68 $cm^3\ g^{-1}$), **Ru-1** (0.59 $cm^3\ g^{-1}$) and **Ru-2** (0.59 $cm^3\ g^{-1}$) are presented in Table 1. A considerable decrease in pore volume was observed (1.16–0.59 $cm^3\ g^{-1}$) after functionalization, immobilization of ligand and further metal complex addition to the calcined SBA-15, indicates the progress of anchoring of the organic moieties inside the channels. But only a small amount of decrease in pore volume was observed after the addition of metal precursors to BzAIL-SBA-15. Pore diameter values of these materials, however, did not change considerably even after functionalization and anchoring of the Ru complexes.

3.3. Solid-state ^{13}C CP MAS NMR spectra

From ^{13}C CP MAS NMR spectra (Fig. 2), one could see the signals at chemical shifts characteristics of the organic moieties attached on the surface of (a) BzCl-SBA-15, (b) Bz-SBA-15 and (c) BzAIL-SBA-15. In the BzCl-SBA-15 (a) a sharp peak at a chemical shift value of 8.6 ppm is assigned to the benzyl-CH_2– fragment present in the functional molecule. The existence of the substituted benzene ring of the functional molecule is identified from the remaining signals at 127.6, 134.3 and 141.2 pp in the spectrum [15]. The persistence

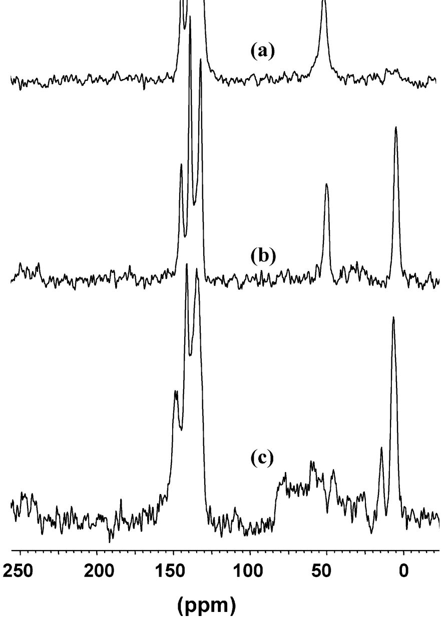

Fig. 2. ^{13}C CP MAS NMR spectra of: (a) BzCl-SBA-15, (b) Bz-SBA-15 and (c) BzAIL-SBA-15.

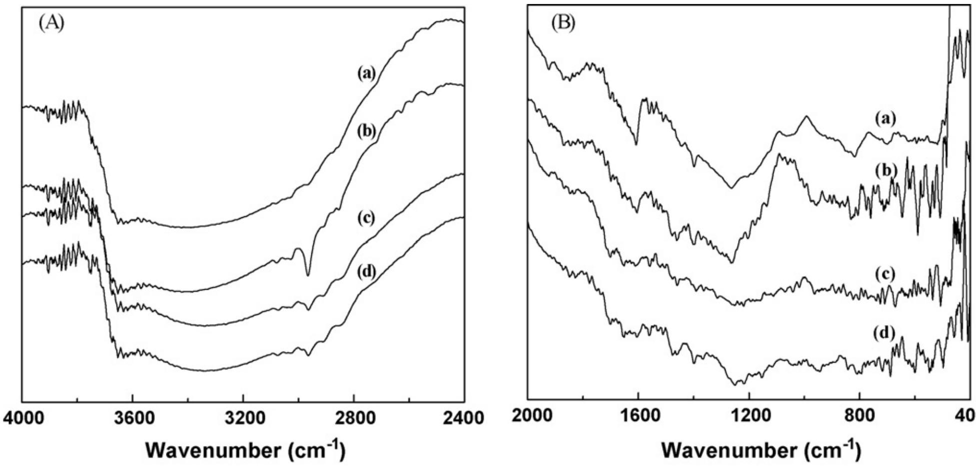

Fig. 3. (A and B). FT-IR spectra of: (a) Bz-SBA-15, (b) BzAIL-SBA-15, (c) **Ru-1** and (d) **Ru-2**.

of the benzyl-CH_2 and benzene ring in Bz-SBA-15 and BzAIL-SBA-15 proved by the presence of the above mentioned peaks in their spectrum. Additionally a sharp peak at 5 ppm evidenced the presence of $-CH_3$ group because of the capping of hydroxyl groups by dimethoxydimethylsilane in Bz-SBA-15. BzAIL-SBA-15 demonstrates a peak at a chemical shift value 10 ppm and a set of peaks in the rang of 39.0–74.0 ppm corresponds to the cyclic $-CH_2$ groups in the immobilized (1*R*,2*S*)-(+)-*cis*-1-amino-2-indanol molecule [16].

3.4. FT-IR study

Fig. 3(A and B) represents the FT-IR spectra of (a) Bz-SBA-15 and (b) BzAIL-SBA-15 (c) **Ru-1** and (d) **Ru-2**. In all the samples a sharp peak at 800 cm^{-1} is due to Si–O stretching band. In addition to the above band, the entire spectra show two weak bands at around 3200–2800 and 1500–1300 cm^{-1} which are due to the C–H stretching and bending vibrations [15] of methylene group of functionalized and ligand molecules. In the ligand immobilized material (BzAIL-SBA-15) we have expected a week band at 3260 cm^{-1} for the –NH stretching vibration, which is unresolved due to the overlapping of O–H stretching vibration (3400 and 3650 cm^{-1}) of surface O–H groups and water molecules occluded in the pores. A small and broad band in all spectrums at 702 cm^{-1} represents the C–H bending vibration of methylene group of benzene [17].

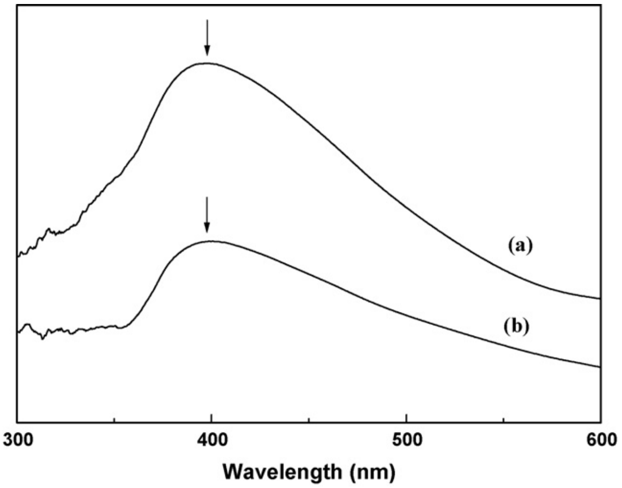

Fig. 4. UV–vis spectra of: (a) **Ru-1** and (b) **Ru-2**.

3.5. UV–vis studies

Fig. 4 illustrates the UV–vis spectra of **Ru-1** (a) and **Ru-2** (b). A sharp peak at 399 nm, which is due to the metal-to-ligand charge-transfer (MLCT) band in both the materials, clearly indicates the successful anchoring of the complex in the surface modified SBA-15 [18].

3.6. Microscopic studies

It is now apparent that morphology and texture of mesoporous silica are extremely important and it may vary with synthesis parameters [19]. Fig. 5 shows the TEM images of calcined SBA-15, along the pore direction (a) and perpendicular to the channels (b). The image (a) clearly revealed the formation of a regular hexagonal array of uniform channels having long-range ordered and the image (b) exposed the formation of well-defined one-dimensional channels. These results further support XRD results presented earlier.

3.7. Asymmetric transfer hydrogenation (ATH) of simple prochiral ketones

In order to elucidate the catalytic activity and enantioselectivity of the synthesized catalysts, the asymmetric transfer hydrogenation reaction of prochiral ketones has performed a procedure similar to the methodology available in literatures for homogeneous chiral amino alcohol complexes. Results are presented in Table 2. All the reactions were carried out under similar conditions in a batch reactor using 2-propanol as solvent as well as proton source. The use of 0.01 mol.% prochiral ketone in conjunction with 0.0001 mol.% of the ruthenium complex (**Ru-1**/**Ru-2)** and 3 mg of KOH in 2-propanol (0.3 ml) at 60 °C temperature resulted in the enantioselective reduction of prochiral ketones to corresponding (*S*)-alcohol. As seen in the Table 2, the heterogeneous catalysts **Ru-1** and **Ru-2** exhibited moderate to good catalytic activity and enantioselectivities for various prochiral ketones like acetophenone, 4-chloroacetophenone, 4-bromoacetophenone, 4-methylacetophenone, 4-methoxyacetophenone, propiophenone and 2,5-dimethoxyacetophenone. Acetophenone reduced 56% and 18% with in 1 h with ee values of 62% and 77% for **Ru-1** and **Ru-2**, respectively (entry 1, Table 2). For instance 4-chloroacetophenone and 4-bromoacetophenone were reduced in 60%, the highest conversion among the substrates, having ee values of 50% and 52% for **Ru-1** (entry 2 and 3, Table 2). But for **Ru-2** catalyst, lower

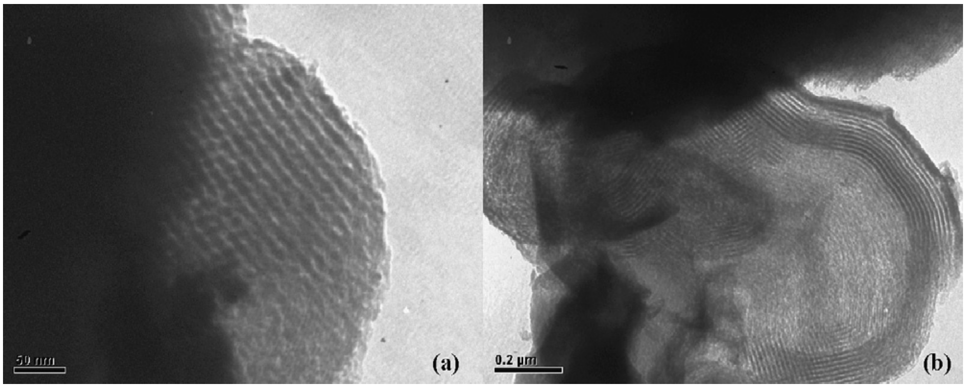

Fig. 5. Transmission electron micrographs (TEM) of SBA-15: electron beam was aligned (a) parallel to the main axis of the channel and (b) perpendicular to the main axis of the channel.

activities (35% and 34%) with enhanced ee values (60% and 62%) have observed (entry 2 and 3, Table 2). The reduction of 4-methylacetophenone gave 33% conversion with 60% ee for **Ru-1** and 19% conversion with 64% ee for **Ru-2** (entry 4, Table 2). 4-Methoxyacetophenone reduced to 52% conversion with 53% ee for **Ru-1** and 21% conversion with 64% ee for **Ru-2** (entry 5, Table 2). 2,5-Dimethoxyacetophenone showed a moderated conversion (43%) and less ee (44%) for **Ru-1** and 14% conversion and 51% ee

Table 2
Asymmetric transfer hydrogenation of simple prochiral ketones

Entry	Substrate	Product	Ru-1		Ru-2	
			Conversion (%)[a]	ee (%)[a]	Conversion (%)[a]	ee (%)[a]
1	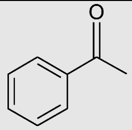	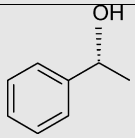	56	62	18	77
2	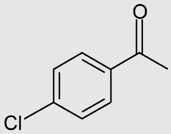	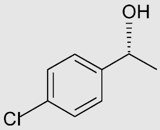	60	50	35	60
3	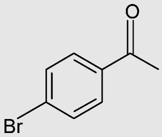	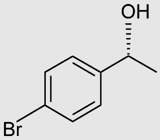	60	52	34	62
4	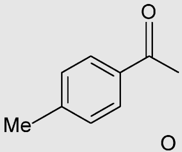	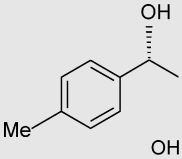	33	60	19	64
5	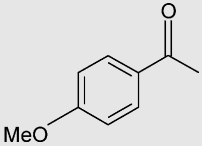	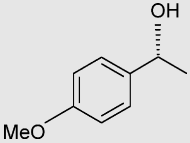	52	53	21	64
6	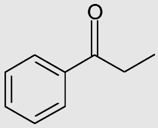	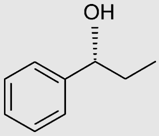	49	54	14	70
7	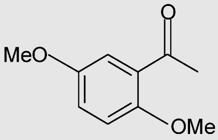	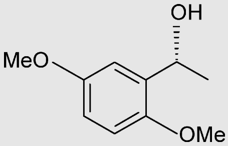	43	44	14	51

The reaction was carried out at 60 °C for 1 h, using 0.01 mol.% of ketone and a S/C ratio of 100 in 3 ml solvent. KOH = 3 mg/0.3 ml 2-propanol. The configuration of alcohol product was *S*.

[a] Determined by GC equipped with a chiral column.

Table 3
Recyclability of the catalysts in the asymmetric transfer hydrogenation of acetophenone

Entry	Cycle	Ru-1		Ru-2	
		Conversion (%)[a]	ee (%)[a]	Conversion (%)[a]	ee (%)[a]
1	Fresh	56	62	18	77
2	First	33	66	11	78
3	Second	13	66	8	77
4	Third	11	64	7	77

The reaction was carried out at 60 °C for 1 h, using 0.01 mol.% of ketone and a S/C ratio of 100 in 3 ml solvent. KOH = 3 mg/0.3 ml 2-propanol.

[a] Determined by GC equipped with a chiral column.

for **Ru-2** (entry 7, Table 2). The low ee of 2,5-dimethoxyacetophenone is probably a result of steric hindrance that affects access of the carbonyl carbon to the Ru(II)-H hydride. Propiophenone exhibited a yield of 49% and ee of 54% for **Ru-1** and 14% yield and 70% ee for **Ru-2** (entry 6, Table 2). From the results, it is observed that the heterogeneous catalyst (**Ru-1**) prepared from $[RuCl_2(\text{benzene})]_2$ displayed higher conversion than the catalyst (**Ru-2**) prepared from $[RuCl_2(p\text{-cymene})]_2$ for simple prochiral ketones. But the ee results are superior for **Ru-2** than **Ru-1** at our reaction conditions and may be due to the favorable special arrangement of sterically hindered *p*-cymene in the metal complex. As a general strategy, the results with the substituted acetophenones suggested that electron-withdrawing groups show higher substrate conversions than electron donating groups. The ee results are exactly reverse to conversion strategy.

In order to ensure the stability and activity of recycled catalysts, we have conducted the recycling study for a maximum of three runs using acetophenone under the similar reaction conditions (Table 3). It is effectively worked out by washing the used catalyst several times with 2-propanol and immediately used for the reaction. Both **Ru-1** and **Ru-2** showed approximately the same ee values at lower conversions. The ICP-AES analysis of the used catalyst after the third run showed a negligible loss of active metal from the catalyst, which attributed the stability of the catalysts even after several recycling.

4. Conclusion

In conclusion, highly reactive heterogeneous catalytic systems were developed by immobilizing (1*R*,2*S*)-(+)-*cis*-1-amino-2-indanol over mesoporous SBA-15 and further complexation with $[RuCl_2(\text{benzene})]_2$ and $[RuCl_2(p\text{-cymene})]_2$. The powder XRD patterns confirm the formation of the siliceous SBA-15 material and the integrity of mesoporous nature throughout the modification process. The N_2 adsorption–desorption studies ascribed the high surface area and considerable pore size distribution, which is in general agreement with previous reports on mesoporous SBA-15. The transmission electron microscopic images strongly supported the XRD and N_2 adsorption–desorption results. ^{13}C CP MAS NMR studies disclosed the unambiguity in anchoring of (4-chloromethyl)phenyltriethoxysilane and (1*R*,2*S*)-(+)-*cis*-1-amino-2-indanol over SBA-15. FT-IR further supported the NMR results. The loading of ruthenium complexes over ligand immobilized SBA-15 has been confirmed by UV–vis analysis and further the amount of active metal was determined by the ICP-AES analysis of **Ru-1** and **Ru-2**. These mesoporous SBA-15 supported chiral catalysts were used for the enantioselective transfer hydrogenation of a range of simple prochiral ketones with moderate to good conversions and enantioselectivity under mild reaction conditions. It is noticed that the substrate having electron withdrawing groups in the para position of the aromatic ring showed higher conversion but a decreased enantiomeric excess it is exactly opposite to the substrates having electron donating groups in their para position. From the comparative reactivity studies of **Ru-1** and **Ru-2**, it is noticed that **Ru-1** is catalytically more active and enantiomerically less selective than **Ru-2**. Acetophenone has given a maximum of 56% conversion and 62% ee for **Ru-1** and 18% conversion and 77% ee for **Ru-2**. The recyclability of the catalysts was effective up to the second recycling step after that an immediate deactivation is observed.

Acknowledgements

S.P. thanks Council of Scientific and Industrial Research, New Delhi for Senior Research Fellowship. The authors are thankful to IFCPAR project for financial support.

References

[1] S. Hashiguchi, A. Fuji, J. Takehara, T. Ikariya, R. Noyori, J. Am. Chem. Soc. 117 (1995) 7562.
[2] Chemical and Engineering News, August, 26, (1996), p. 25.
[3] P.N. Liu, J.G. Deng, Y.Q. Tu, S.H. Wang, Chem. Commun. (2004) 2070.
[4] P.N. Liu, P.M. Gu, F. Wang, Y.Q. Tu, Org. Lett. 6 (2) (2004) 169.
[5] J. Takehara, S. Hashiguchi, A. Fujii, T. Ikariya, R. Noyori, Chem. Commun. (1996) 233.
[6] M. Palmer, T. Walsgrove, M. Wills, J. Org. Chem. 62 (1997) 5226.
[7] D.A. Alonso, D. Guijarro, P. Pinho, O. Temme, P.G. Andersson, J. Org. Chem. 63 (1998) 2749.
[8] T. Bein, Curr. Opin. Solid State Mater. Sci. 4 (1999) 85.
[9] E. Breysse, C. Pinel, M. Lemaire, Tetrahedron Asymmetry 9 (1998) 89.
[10] D.J. Bayston, C.B. Travers, M.E.C. Polywka, Tetrahedron Asymmetry 9 (1998) 2015.
[11] A.J. Sandee, D.G.I. Petra, J.N.H. Reek, P.C.J. Kamer, P.W.N.M. van Leeuwen, Chem. Eur. J. 7 (6) (2001) 1202.
[12] M.A. Bennett, A.K. Smith, J. Chem. Soc., Dalton Trans. (1974) 233.
[13] D. Zhao, J. Feng, Q. Huo, N. Melosh, G.H. Fredrickson, B.F. Chmelka, G.D. Stucky, Science (Washington, DC) 279 (1998) 548.
[14] M. Jia, A. Seifert, W.R. Thiel, Chem. Mater. 15 (2003) 2174.
[15] D. Jiang, Q. Yang, H. Wang, G. Zhu, J. Yang, C. Li, J. Catal. 239 (2006) 65.
[16] M. Kinugasa, T. Harada, A. Oku, Tetrahedron Lett. 39 (1998) 4529.
[17] M. Suzuki, S. Ito, T. Kuwahara, Bull. Chem. Soc. Jpn. 56 (1983) 956.
[18] R.J. Staniewicz, R.F. Sympson, D.G. Hendricker, Inorg. Chem. 16 (1977) 2166.
[19] K. Kosuge, T. Sato, N. Kikukawa, M. Takemori, Chem. Mater. 16 (2004) 899.